Atomic Structure of the Polar NiO(111)-$p(2 \times 2)$ Surface

A. Barbier,[1,*] C. Mocuta,[1] H. Kuhlenbeck,[2] K. F. Peters,[3] B. Richter,[2] and G. Renaud[1]
[1]*CEA/Grenoble, Département de Recherche Fondamentale sur la Matière Condensée SP2M/IRS,*
17, Rue des Martyrs, 38054 Grenoble Cédex 9, France
[2]*Fritz-Haber-Institut der Max-Plack-Gesellschaft, Faradayweg 4-6, D-14195 Berlin, Germany*
[3]*ESRF, BP 220, 38043 Grenoble Cedex, France*
(Received 9 September 1999)

Using grazing-incidence x-ray diffraction, the $p(2 \times 2)$ surface structures of the single crystal NiO(111) and a 5 monolayer thick NiO(111) film on Au(111) were both shown to exhibit locally the theoretically predicted octopolar reconstruction, with some important differences. The single crystal exhibits a single Ni termination with double steps. The thin film exhibits both possible terminations (O and Ni) and single steps. These surfaces were found to be nonreactive with respect to hydroxylation.

PACS numbers: 68.35.Bs, 61.10.–i

The electrostatically polar (111) surfaces of the rocksalt oxides (NiO, CoO, MnO, and MgO) remain mysterious, because they are difficult to investigate both experimentally and theoretically [1–3]. Since the bulk structure has alternating cationic and anionic sheets along the [111] direction, the simple truncated surfaces must have a divergent electrostatic energy, in theory making them highly unstable. Thus, the polar rocksalt surfaces were long believed to be unstable, according to Tasker [4] and to an early experimental evidence of (100) faceting on MgO(111) [5]. Their technological importance is growing because of their very particular properties, e.g., in catalysis [6]. Also, the (111) plane of NiO may perform exchange coupling of ferromagnetic films [7] in the newest giant magnetoresistive sensors [8].

Wolf recently predicted that such surfaces may be stabilized by a particular $p(2 \times 2)$ "octopolar" reconstruction (Fig. 1), which cancels the divergence of the electric field in the crystal [9]. Indeed, NiO(111) surfaces do exist as facets on small NiO single crystals [10] and as thin films with a $p(2 \times 2)$ structure [11,12], and we have shown how to prepare single crystal surfaces without decomposition [13]. A reanalysis of the initial findings on MgO(111) shows that the (100) facets were, in fact, vicinal (111) surfaces [14,15], but the proposed structural model is very different from Wolf's one and other predicted models for MgO(111) [16]. Early experiments on NiO(111) also showed complex reconstructions attributed to Si segregation [17]. Thus the real structure of polar oxide surfaces and the importance of the electrostatic criterion are still uncertain. The possibility to produce NiO(111) surfaces of high crystalline quality and known structure should open new possibilities for theorists and experimentalists in the fields of highly correlated materials [18], magnetism [19–21], and catalysis [6].

In the present paper, we describe the first comparative structure determination of NiO(111) surfaces on both a single crystal and a thin NiO(111) film. Glancing-incidence x-ray diffraction (GIXD) is used, because it is well suited to investigate metal/oxide interfaces since it is not hampered at all by the charge buildup [22,23]. All the experiments reported here were performed on the ID03 surface diffraction beam line [24] at the ESRF (European Synchrotron Radiation Facility, Grenoble, France) in ultrahigh vacuum conditions (10^{-10} mbar). Measurements were performed on the single crystal surface at 18 keV photon energy and at the 0.17° critical incidence angle for total external reflection to reduce the scattering from the bulk. The thin film surface was measured at 17 keV and 0.9° incidence angle, because the bulk scattering from the Au(111) substrate was weak in the regions of interest.

To measure the weak scattering from the octopolar reconstruction above the bulk signal of NiO(111) single

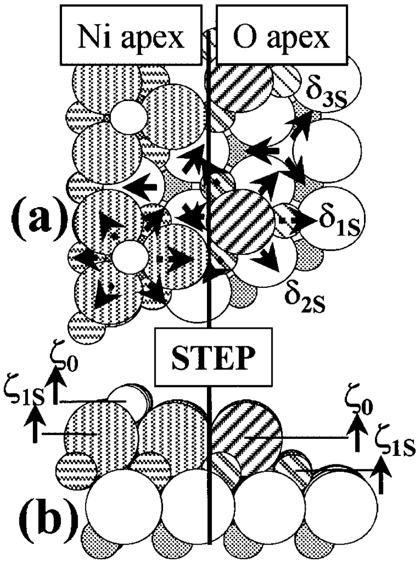

FIG. 1. (a) Top and (b) side views of two possible octopolar reconstructions with Ni- or O-terminated terraces (left and right, respectively), separated by a single step (solid line). Large circles are oxygen atoms, and small circles are nickel. For either termination, the top two layers are 75% and 25% vacant compared to the bulk lattice. The possible symmetry-compatible relaxations, δ and ζ, are shown as arrows indicating a positive relaxation.

0031-9007/00/84(13)/2897(4)$15.00 © 2000 The American Physical Society

crystals, an improved crystal preparation was needed. Commercial wafers [25] do not meet the requirements due to the large angular misorientations (up to 2°) between grains called mosaicity or mosaic spread [22,23]. Annealing in air at 1300 K reduces the mosaicity to 0.7°, preserves the surface morphology, and reveals only the first-order reflection of the reconstruction [13,26]. Annealing to 1700 K further reduces the mosaicity but the surface morphology deteriorates. In the present study, high quality surfaces with good morphology were obtained by annealing the NiO boule at 1850 K for 24 h in air, then cutting, polishing, and reannealing at 1300 K for 3 h, which yields a flat, shiny surface. A mosaicity of 0.054° and a typical domain size (usually interpreted as the mean terrace size) of 1800 Å are obtained. Such crystals have high crystalline quality up to the surface and are well suited for GIXD investigations [17]. In the vacuum chamber, the surface is $p(2 \times 2)$ reconstructed with some residual C and sometimes Ca. GIXD data were taken after such an *ex situ* sample preparation because further treatments proved ineffective. Annealing under up to 10^{-4} mbar O_2 at 700 K removes the C contamination but drastically transforms the internal structure of the reconstruction. An O_2 sputtering at 2 keV and an anneal in air at 1000 K removes the Ca contamination but leaves a large mosaicity, making a complete analysis impossible. Nonetheless, since the first orders of the reconstruction retain the same relative intensities, the Ca is neither responsible for the reconstruction nor for its internal structure. Thus, our *ex situ* preparation has given the best surface.

The NiO(111) thin film was prepared *in situ* on Au(111) [11,12,28]. The surface used for the growth had a mosaicity of 0.052° and a domain size of 2600 Å exhibiting the herringbone reconstruction [29]. During deposition the substrate was held at 615 K, and the Ni was evaporated from an electron-bombarded Ni rod in a 2×10^{-5} mbar partial pressure of O_2. A perfect 2D growth has been observed from 3 to 8 monolayers (ML) before 3D crystallites formed. For the quantitative analysis we have chosen an intermediate thickness of 5 ML. The NiO(111) thin film was in good epitaxy, of good crystalline quality, completely relaxed, and $p(2 \times 2)$ reconstructed with 0.106° mosaicity, 550 Å domain size, and intense throughout the accessible region of reciprocal space.

Following convention, the crystallographic basis vectors for the surface unit cell describe the triangular lattice of the reconstruction. They are related to the bulk basis by $\mathbf{a}_{\mathrm{surf}} = [\bar{1}10]_{\mathrm{bulk}}$, $\mathbf{b}_{\mathrm{surf}} = [0\bar{1}1]_{\mathrm{bulk}}$, and $\mathbf{c}_{\mathrm{surf}} = [111]_{\mathrm{bulk}}$. The h and k indexes are chosen to describe the in-plane momentum transfer [in reciprocal lattice units, r.l.u., of the NiO(111) reconstruction], and L the perpendicular momentum transfer. We have never observed any periodicity other than $p(2 \times 2)$.

The in-plane scattering of the $p(2 \times 2)$ patterns was measured quantitatively by rocking scans at all accessible positions belonging to the reconstruction. For the single crystal, 33 nonzero peaks were measured at $L = 0.1$. The symmetry of the diffraction pattern is $P6mm$ leaving 14 nonequivalent peaks with a systematic uncertainty of 12%. For the thin film 59 nonzero peaks were measured at $L = 0.3$ and the diffraction pattern has $P3m1$ symmetry, leaving 32 nonequivalent peaks with a systematic error level of 11%. The largely different symmetries cannot be explained by the small L difference but is rather due to different $p(2 \times 2)$ structures.

For the single crystal, the measured and calculated in-plane scattering can be directly compared, using the octopolar model with both Ni and O termination. Reproducing the crystal truncation rods (CTR) restricted the solution to the Ni termination uniquely, plus the following symmetry-related atomic relaxations in each atomic layer p ($p = 0$ for the apex layer of atoms). Note that three of the four atoms in layer p of the unit cell have symmetry-related vertical displacements ζ_{pS}, whereas the independent atom has vertical displacement ζ_p. Likewise, δ_{pS} defines a radial displacement of symmetry-related atoms away from the in-plane position of the apex atom (Fig. 1). The ρ_{pS} terms define the possible rotational displacements. Detailed fitting reveals that all δ_{pS} and ρ_{pS} terms are negligible except $\delta_1 = 0.117 \pm 0.015$ Å, which indicates a dilatation of the threefold hollow site where the apex atom rests. The least-squares refinement converges for a 0.2 Å rms roughness, $\zeta_0 = 0.06 \pm 0.02$ Å, $\zeta_{1S} = -0.17 \pm 0.02$ Å, $\zeta_2 = 0.13 \pm 0.01$ Å, $\zeta_{2S} = -0.029 \pm 0.007$ Å, $\zeta_3 = 0.23 \pm 0.12$ Å, $\zeta_{3S} = -0.09 \pm 0.02$ Å, $\zeta_4 = 0.02 \pm 0.01$ Å, and $\zeta_{4S} = -0.005 \pm 0.003$ Å. For the 138 structure factors a global χ^2 of 1.5 is obtained with nine structural parameters, the roughness, and a scale factor. The agreement is good [Figs. 2, 3(a)]; further relaxations do not significantly improve the fit. The relaxations extend deeply into the crystal. The smallest bond length in the refined model is 1.9 Å, i.e., a 10% contraction, and is located between the last complete layer ($p = 2$) and the 25% vacant layer of the octopole ($p = 1$). The same procedure with an O-terminated surface does not converge and the best χ^2 was 30. Other recently proposed models for MgO [14,30] were also tested but were unable to reproduce our data ($\chi^2 \approx 15$), even with relaxations. The present CTRs are almost identical to previously measured CTRs on an apparently unreconstructed surface [13,26]. They could not be reproduced with a (1×1) surface, and a contamination was proposed [26]. It is now clear that the surface was reconstructed and Ni terminated, but the large mosaicity make the weak reconstruction peaks unmeasurable.

For the thin film, the octopolar reconstruction cannot reproduce the in-plane data, regardless of the relaxations. The out-of-plane periodicity, seen in 13 diffraction rods with 322 nonzero structure factors, indicates a 3 layer thick reconstruction.

A coherent juxtaposition of half Ni- and half O-terminated domains separated by single steps yields the experimental Patterson map (provided that the bases of the two octopoles have the same orientation). The structure was refined, as for the single crystal, using the same relaxations plus a domain fraction, the roughness, and a scale factor. Note the identical relaxations in the two domains so that ζ_0 is the perpendicular relaxation of both apex atoms, and so on (Fig. 1). The best stable solution remained essentially unchanged when we allowed independent relaxations in the two domains. Only three relaxations were non-negligible. The best agreement was obtained for $\delta_{1S} = 0.096 \pm 0.008$ Å, $\delta_{2S} = 0.078 \pm 0.007$ Å, and $\zeta_0 = -0.103 \pm 0.028$ Å, with 50% Ni- and 50% O-terminated domains, a 1 Å roughness and with a global χ^2 of 1.4. This solution reproduced well all the data. It is worth noting that other models containing the two terminations over bulklike layers might also be able to reproduce the data, but we have not found any acceptable alternatives within a growth process.

Figure 2 compares the experimental and calculated in-plane structure factors for both the single crystal and the thin film. Some typical rods are shown in Fig. 3(b). The agreement is very good up to large momentum transfers, definitively supporting this two-variant octopolar reconstruction. Note that, contrary to double steps, the single step belongs to the model itself and will thus not influence the coherence length (550 Å), i.e., the single steps may be located anywhere and have not necessarily formed large continuous step edges.

Let us now discuss these results. Obviously, Wolf's octopolar reconstruction is the basic stone needed for the interpretation of both data sets. In both cases, the relaxations are small and resemble one another, thus leaving them close to the theoretical octopolar reconstruction on a local scale, at least. The single crystal result with double steps separating Ni-terminated domains indicates that Ni termination is likely the equilibrium octopolar reconstruction.

The x-ray data show the thin film can adopt both terminations and therefore single steps, as well. This model appears to contradict a scanning tunneling microscopy (STM) study on a NiO film, where double steps were observed to separate adjacent domains [11]. Unfortunately, the authors did not systematically report on the populations of single versus double steps or the populations of the two octopolar terminations. Since a perfect octopolar reconstruction consists of a 25% vacant layer with 25% adatoms of the other species, near-atomic resolution might be needed to identify single steps among the other possible defects in the images. Double steps are more easily identifiable in STM. By comparison, the x rays clearly see both terminations, via the in-plane and the out-of-plane scattering. Note that since the single steps are intrinsic to the model and do not determine the coherence length, the data do not determine the single-step morphology, e.g., as separating large terraces or small islands.

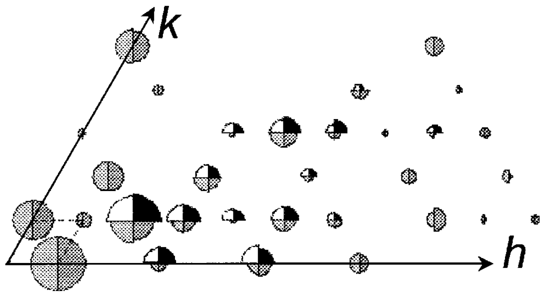

FIG. 2. Comparison between the measured in-plane structure factors (right) and calculated ones (left) for the octopolar reconstruction for the single crystal with Ni apex (top when the reflection was measured) and the thin film compared to the two-domain octopolar reconstruction (bottom and complete circles).

We note that the thin film was grown under nonequilibrium conditions. At 615 K, Ni has a limited mobility on NiO, since Ni clusters appear only at higher temperatures on NiO [13,31]. The atomic flux ratio was roughly 1000:1 of O:Ni onto the surface. For these reasons, the growing surface necessarily passes through nonequilibrium structures in order to fill the incomplete lower layers. Figure 4 shows how a perfect Ni-terminated octopolar domain (as inside the dotted circle) could be transformed to O termination (as the dashed circle) via incorporation of a half-monolayer of Ni at sites A and B, plus oxygen atoms C and D. We propose that the observed O-terminated regions are relatively stable metastable domains that are achieved during the special conditions of growth. It would be interesting to monitor the film growth via *in situ* GIXD.

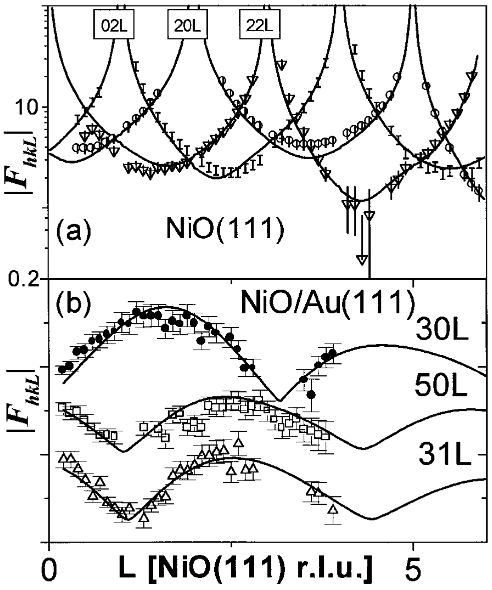

FIG. 3. (a) Measured 20 L (○), 22 L (▽), and 02 L (I) NiO(111) CTRs compared with a relaxed Ni-terminated octopolar reconstruction (straight lines). (b) Comparison of measured and calculated diffraction rods of the $p(2 \times 2)$ reconstruction of a 5 ML thick NiO(111) film grown on Au(111). The h and k indexes are expressed in the (2×2) r.l.u.

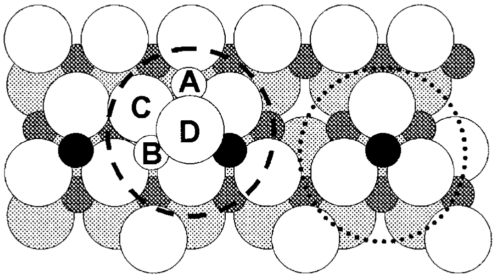

FIG. 4. Schematic representation of the growth of an O-terminated octopole (dashed circle) on top of a Ni apex (dotted circle) terminated surface by addition of 2 Ni (*A* and *B*) and 2 O (*C* and *D*) atoms. Small circles are Ni atoms, whereas large circles stand for O atoms.

Since Au does not easily oxidize, we can assume that the interfacial layer is Ni. Ni- and O-terminated octopolar structures are electrostatically equivalent. For the thin film, each Au(111) step will place unlike layers at the same height, causing an accumulated electrostatic energy that may be responsible for the sudden change from two- to three-dimensional growth after 8 ML.

The stability of both surfaces against hydroxylation was tested by extensively dosing the surface with up to 10^6 L [1 L (langmuir) $= 10^6$ Torr s] of H_2O at 3×10^{-5} mbar partial pressure at room temperature. No structural effect could be detected. For the single crystal, the octopolar reconstruction is stable in air. Previously, NiO(111) films of poor structural quality made by oxidation of Ni(111) [12,30] were found unstable against hydroxylation. We thus suggest that the reactivity of NiO(111) against water mainly takes place at defects (like for MgO [32]), which are almost absent on our surfaces.

Our main conclusion is that NiO(111) is terminated by a nearly ideal octopolar reconstruction, as Wolf theoretically predicted. The Ni octopolar termination is stable on the single crystal, but thin film growth can produce O termination too. Moreover the electrostatic driving force is strong enough to stabilize the surface reconstruction even in air or water (only metallization seems to be more stable). The extent to which these results can be extrapolated to other polar oxide surfaces or thin films is still an open issue that may only be solved once the preparation conditions of the corresponding crystals are determined.

The ID03 beam line staff from the ESRF is gratefully acknowledged for assistance and very good experimental conditions. C. A. Ventrice, H.-J. Freund, A. Stierle, and P. Humbert are acknowledged for fruitful discussions and E. Vlieg for providing the ROD software.

---

*Corresponding author.
Email address: abarbier@cea.fr

[1] J. J. M. Pothuizen, O. Cohen, and G. A. Sawatzky, Mater. Res. Soc. Symp. Proc. **401**, 501 (1996).
[2] V. I. Anisimov, F. Aryasetiawan, and A. I. Lichtenstein, J. Phys. Condens. Matter **9**, 767 (1997).
[3] P. M. Oliver, G. W. Watson, and S. C. Parker, Phys. Rev. B **52**, 5323 (1995), and references therein.
[4] P. W. Tasker, J. Phys. C **12**, 4977 (1979).
[5] V. E. Henrich, Surf. Sci. **57**, 385 (1976).
[6] D. Cappus *et al.*, Chem. Phys. **177**, 533 (1993).
[7] W. H. Meiklejohn, J. Appl. Phys. **33**, 1328 (1962).
[8] S. Soeya, S. Nakamura, T. Imagawa, and S. Narishige, J. Appl. Phys. **77**, 5838 (1995), and references therein.
[9] D. Wolf, Phys. Rev. Lett. **68**, 3315 (1992).
[10] J. M. Cowley, Surf. Sci. **114**, 587 (1982).
[11] C. A. Ventrice, Jr., Th. Bertrams, H. Hannemann, A. Brodde, and H. Neddermeyer, Phys. Rev. B **49**, 5773 (1994).
[12] F. Rohr, K. Wirth, J. Libuda, D. Cappus, M. Bäumer, and H. J. Freund, Surf. Sci. **315**, L977 (1994).
[13] A. Barbier and G. Renaud, Surf. Sci. Lett. **392**, L15 (1997).
[14] R. Plass, K. Egan, C. Collazo-Davila, D. Grozea, E. Landree, L. D. Marks, and M. Gajdardziska-Josifovska, Phys. Rev. Lett. **81**, 4891 (1998).
[15] R. Plass, J. Feller, and M. Gajdardziska-Josifovska, Surf. Sci. **414**, 26 (1998).
[16] A. Pojani, F. Finocchi, J. Goniakowski, and C. Noguera, Surf. Sci. **387**, 354 (1997).
[17] N. Floquet and L.-C. Dufour, Surf. Sci. **126**, 543 (1983).
[18] M. Finazzi, N. B. Brookes, and F. M. F. de Groot, Phys. Rev. B **59**, 9933 (1999).
[19] G. Ju, A. V. Nurmikko, R. F. C. Farrow, R. F. Marks, M. J. Carey, and B. A. Gurney, Phys. Rev. B **58**, R11 857 (1998).
[20] J. P. Hill, C.-C. Kao, and D. F. McMorrow, Phys. Rev. B **55**, R8662 (1997).
[21] V. Fernandez, C. Vettier, F. de Bergevin, C. Giles, and W. Neubeck, Phys. Rev. B **57**, 7870 (1998).
[22] G. Renaud, Surf. Sci. Rep. **32**, 1 (1998).
[23] I. K. Robinson and D. J. Tweet, Rep. Prog. Phys. **55**, 599 (1992), and references therein.
[24] ESRF beam line handbook (http://www.esrf.fr).
[25] Wafers were of outside diameter (∅) 12 mm, 1 mm thick, purity 99.9% made of NiO powders with 99.99% purity provided by Crystal GmBH, Berlin, Germany.
[26] A. Barbier, G. Renaud, and A. Stierle, Surf. Sci. **402–404**, 757 (1998).
[27] Importantly, this procedure also avoids the commonplace formation of a magnetically "dead" layer, which we now understand is due to a surface composition change due to polishing (unpublished results).
[28] The Au(111) single crystal (∅ 13 mm, 3 mm thick) was provided by—and polished at—the Fritz-Haber Institute, Berlin, Germany.
[29] A. R. Sandy, S. G. J. Mochrie, D. M. Zehner, K. G. Huang, and Doon Gibbs, Phys. Rev. B **43**, 4667 (1991).
[30] N. Kitakatsu, V. Maurice, and P. Marcus, Surf. Sci. **411**, 215 (1998).
[31] A. Barbier, G. Renaud, C. Mocuta, and A. Stierle, Surf. Sci. **433–435**, 761 (1999).
[32] Ping Liu, Tom Kendelewicz, and Gordon E. Brown, Jr., Surf. Sci. **412**, 315 (1998).